Received: 25 August 2023 | Revised: 5 December 2023 | Accepted: 9 December 2023

DOI: 10.1002/pc.28048

RESEARCH ARTICLE

Polymer COMPOSITES WILEY

Wear-resistant layers containing graphene derivatives

Ferda Mindivan[1] | **Hilal Dere**[2]

[1]Faculty of Engineering, Department of Bioengineering, Bilecik Seyh Edebali University, Bilecik, Turkey

[2]Faculty of Engineering, Department of Mechanical Engineering, Bilecik Seyh Edebali University, Bilecik, Turkey

Correspondence
Ferda Mindivan, Faculty of Engineering, Department of Bioengineering, Bilecik Seyh Edebali University, Bilecik, 11100, Turkey.
Email: ferda.mindivan@bilecik.edu.tr

Funding information
Bilecik Şeyh Edebali University, Grant/Award Number: 2020-02. BŞEÜ.03-04

Abstract

The effect of carbon filler wt% ratios on the microstructural and tribological properties of the ultra-high molecular weight polyethylene (PE)/graphene nanoplatelets (GNP), PE/graphene oxide (GO), and PE/carbon nanotube (CNT) composites and PE/GNP-GO hybrid composite layers was studied to determine the best tribological performance after the dry wear test. The layers had a semi-crystalline structure like PE, but the shifts in the peaks showed the presence of interactions between the fillers and PE matrix, according to x-ray diffraction (XRD) analysis. FTIR analysis results indicated that GO-containing layers caused interactions and new bonds. The lowest values for the friction coefficient were found in layers containing GNP and GO, which had a lubricating effect. The friction coefficient decreased by 83.24% in the PE/0.7GO composite layer compared to PE. Wear resistance of the PE/3GNP and PE/1GO layers were the highest compared to PE and other layers. The PE/3GNP and PE/1GO layers improved the wear resistance of PE by 12% and 11%, respectively. Abrasive wear and fatigue wear tracks on the worn surface of the PE/3GNP and PE/1GO composite layer were significantly reduced compared to PE and other layers. This study suggests that layers that will provide the highest molecular interaction with PE and improve its wear resistance will be produced with GO and nano-sized GNP.

Highlights

- The interaction of graphene-derived fillers with PE and its effect on friction and wear properties were investigated.
- GNP and GO are the best filler materials among the graphene derivatives for increasing wear resistance.
- High wear resistant of layers achieved at 3 wt% GNP loadings.
- Layers containing GO had the lowest friction coefficient values among the other layers.

KEYWORDS

carbon nanotube, graphene nanoplatelets, graphene oxide, wear-resistant

1 | INTRODUCTION

Ultra-high molecular weight polyethylene (PE) is an engineering thermoplastic and the material of choice for bearing components in hip and knee total joint arthroplasty.[1] PE has great chemical stability, good self-lubricating qualities, good wear resistance, and low friction. It is also biocompatible.[2] Three million joint

replacement procedures are performed worldwide each year, and PE is typically used in these procedures. However, orthopedic implants have a restricted lifetime.[3] Wear of PE fragments leads to osteolysis,[4] and it has disadvantageous properties such as low surface hardness and anti-fatigue capacity.[5] Therefore, the improvement of the mechanical properties and wear resistance of neat PE is highly prominent.[6] Incorporating fillers to overcome the deficiency of the PE matrix is a hopeful solution. For this purpose, some researchers developed composite materials with PE matrices that were produced using various inorganic and organic fillers.[7] Unfortunately, the use of fillers in artificial joints was limited due to poor performance, high cost, and high additive amounts of composites.[5] In this study, graphene nanoplatelets (GNP), graphene oxide (GO), and carbon nanotube (CNT) fillers, which are some carbon derivatives, were used in the PE matrix. Recent research has focused on graphene as a possible filler due to its high surface area, potential for strong bonding, and efficient load transmission between the filler and polymer matrix.[8] Graphene nanoplatelets (GNP) have properties closer to those of single-layer graphene than other graphene derivatives.[9] Furthermore, a 2D graphene layer improves lubrication properties and promotes more homogeneous filler dispersion in the polymer matrix.[10] To investigate the mechanical and tribological properties of PE composites with GNP, numerous tests are being carried out. Wang et al.[11] investigated the electrical conductivity of PE/graphene nanosheet composites. According to the study of Aliyu et al.,[12] PE composites with low GNP contents (0.1, 0.25, and 0.5 wt %) were produced, and the results revealed that PE/0.25 wt% GNPs had the maximum wear resistance. Chih et al.[13] prepared spray-coated UHMWPE composites with 0–4.6 wt% of GNP and 1–2 layered graphene (2LG). Test results indicated that GNP presented better tribological behavior than 2LG. Alam et al.[8] reported at the thermal, mechanical, and electrical characteristics of PE nanocomposites with graphene nanoplatelets. Gu et al.[1] presented the thermal conductivity of graphite nanoplatelet/UHMWPE nanocomposites, and these were fabricated via mechanical ball milling followed by a hot-pressing method. Unlike all this literature, in this study, composite layers were produced with higher GNP contents and lower particle thicknesses of GNP. As a consequence, the tribological and structural properties of composite layers can be altered by changing the loading content of GNP. Moreover, GNP may be a good candidate to overcome the wear defects of the PE.[14] GO is obtained by the oxidation of graphite. GO has functional groups that include hydroxyl, carboxyl, and epoxy groups. The oxygen-containing functional groups disperse easily into some polar solvents and form intercalated composites owing to their strong interaction with polar molecules.[15–17] An et al.[6] reported that pure PE and its composites were produced with different GO wt% (0,1, 0.3, 0.7, and 1.0) by liquid phase dispersion, ball mill mixing at high speed, and hot pressing and showed an improvement in the wear resistance of the composites. Pang et al.[5] studied the mechanical and thermal properties of GO/PE nanocomposites. The results showed that the thermal and mechanical properties of nanocomposites improved with increasing GO content. In the studies of Chen et al.,[16] GO/PE composites were produced by liquid-phase dispersion followed by hot pressing. They investigated the microstructural, mechanical, and biocompatibility properties of composites formed by the addition of pure PE and different wt% (0.1, 0.3, 0.5, and 1.0) GO. CNTs have been extensively used because of their good mechanical, electrical, and thermal properties.[18] CNTs have unique properties such as high elastic modulus (200–1000 GPa), tensile strength (11–63 GPa), and good lubricity.[19,20] CNTs with a maximum tensile strength of 300 GPa are highly durable materials.[18] In the studies of Zoo et al.,[21] CNT was added to the PE matrix at different wt% (0.1, 0.2, and 0.5) to improve the tribological properties of PE. The results showed that CNT was a potential filler material to increase wear resistance without significant structural changes. Samad and Sinha[22] produced composite materials with the addition of plasma-treated SWCNT at different wt% (0.05, 0.1, and 0.2) to improve the mechanical, thermal, and tribological properties of PE layers on DF3 tool steel backing material. SWCNTs contributed to the improvement of the mechanical and thermal properties of the film without causing any structural changes in the polymer matrix. From the results of the studies summarized in the literature above, it was understood that GNP, GO, and CNT fillers had significant effects on the structural, thermal, mechanical, and tribological properties of the PE composite and nanocomposite materials. In this study, GNP, GO, and CNT powders, which are known as carbon-derived filler materials, were applied to the PE matrix with different wt% ratios. Composite powders (PE/GNP, PE/GO, and PE/CNT) and hybrid composite powder mixtures (PE/GNP-GO) were produced by mixing with the liquid phase dispersion method in wt% values. These powders were coated onto PE with the hot press molding process. The reason for using composite layer instead of composite is that the cost of producing numerous filling materials for industrial applications increases. Therefore, composite powder is more advantageous. Furthermore, the effect of filler wt% ratios on the microstructural and tribological properties of the produced composite and hybrid composite layers was studied. Wear tests were performed on the layers in dry sliding conditions. In this

study, it was aimed at determining the composite or hybrid composite layer that offered the best tribological performance after the wear test.

2 | MATERIALS AND METHODS

PE used in the present work was from Sigma-Aldrich Chemie. The molecular weight was in the range of 3–6 million as per the manufacturer's data. The powder's density was 0.94 g/mL. Graphene nanoplatelets (GNPs) were purchased from Graphene Chemical Industries Co. with an average particle thickness of 5–8 nm. Powder thickness was 5 μm, and surface area was 120–150 m^2/g. The Hummers method[23] was used to prepare GO from graphite. CNT powders with a particle size of 9.5 nm in diameter, 1.5 μm in length, and surface area was 250–300 m^2/g. It was purchased from Graphene Chemical Industries Co. Before preparing the composite mixture, the surface of the CNT was modified. CNT powders were washed in a HNO_3/H_2SO_4 (1:1 volume) acid mixture in an ultrasonic bath at 80°C with distilled water until the pH was 5.0, and then dried in an oven at 100°C for 24 h.

PE composites and hybrid powders of different weight percentages (wt%) of GNP, GO, CNT, and GO-GNP in PE were prepared as follows: In brief, fillers were sonicated for 30 min in ethanol using an ultrasonic bath. Ultrasonic mixing provides better distribution of powders in the ethanol solution and PE solution compared to mechanical mixing. Ultrasonic mixing is used in studies on graphene derivatives in the literature.[12,15] The filler suspension was then combined with PE powders, and the mixture was mixed for 30 min before being sonicated for an hour. After that, the composite powders were dried in an oven at 60°C after the ethyl alcohol was removed at 60–70°C in an oil bath. The final step was hot pressing composite powders onto PE for 30 min at 180°C and 10 MPa pressure.[24] The composite and hybrid layers were coded by their wt% GNP, GO, CNT, and GO-GNP in PE. The images and molecular representations of the layers were given in Figures 1 and 2.

X-ray diffractograms (XRD) obtained by a PAN analytical, empyrean diffractometer employing Cu K radiation in the angle range $2° = 5°–30°$ served as a representation of the crystallinity of the layers. The

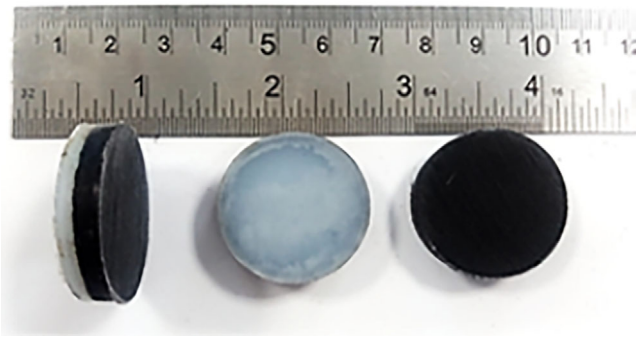

FIGURE 1 The images of layers.

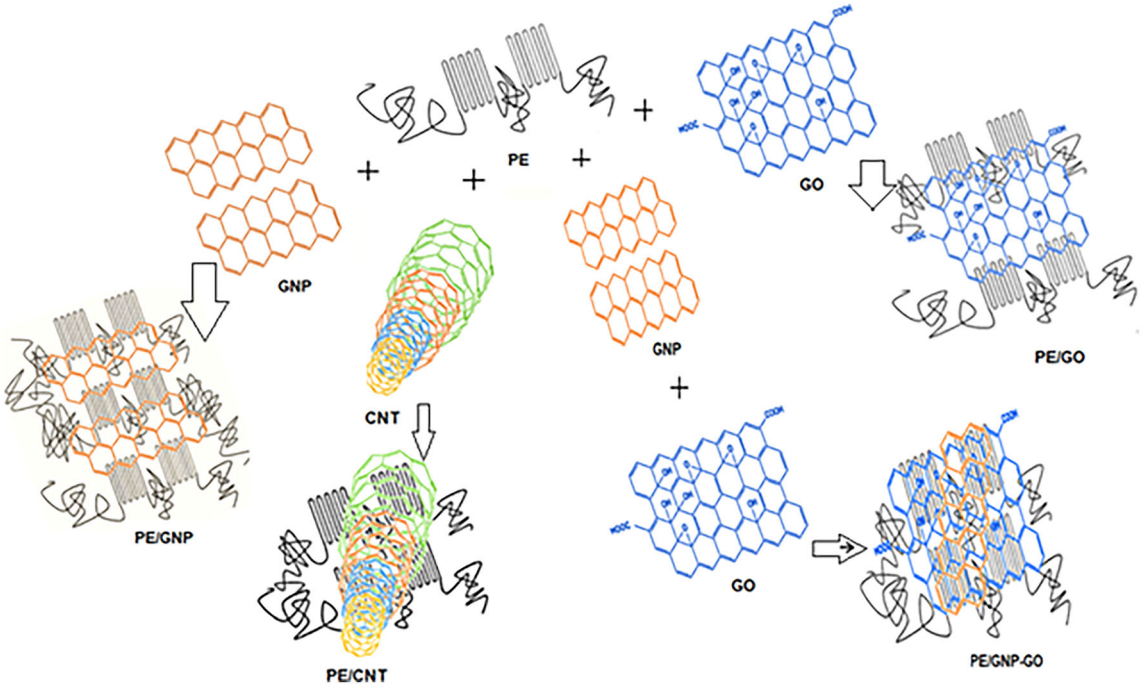

FIGURE 2 Molecular representations between PE and GO, CNT and GNP.

crystallite size of the layers was calculated by the following Scherrer Equation (1).[25,26]

$$L = \frac{k.\lambda}{\beta.\cos\theta} \quad (1)$$

where L is the crystallite's size, K is a shape-related constant, lambda is the width at half its maximum, beta is the wave's length, and theta is the peak location.

The molecular structure of the composite layers was characterized by Fourier transfer infrared spectroscopy (FTIR) spectra, which are recorded by a Spectrum 100, Perkin Elmer, between 400 and 4000 cm^{-1}. We obtained transmission electron microscope (HR-TEM) images of the cross-section area of the PE/3GNP layer using Jeol 2100F 200 kV RTEM to explain the distribution of GNP at the interface. The tribological properties of the obtained layers were investigated using a reciprocating wear tester under dry sliding conditions (Figure 3). The outside temperature was about 25°C, and the relative humidity was nearly 45%. The wear tests on all layers were performed under a constant load of 5 N using a 5 mm-diameter 316 L ball at a sliding velocity of 1.9 cm/s over a sliding distance of 57.5 m. The wear was calculated by analyzing the width and depth of wear scars developing on layer surfaces with the help of a contact stylus profilometer (SJ400). The wear rate was calculated using Equation (2).

$$A = \frac{\pi.W.D.C}{4.S.F} \quad (2)$$

where A: Wear rate, mm^3/Nm. W: Width of wear scar, mm. D: Depth of wear scar, mm. C: Length of wear scar, mm. S: Total sliding distance, m. F: The test load is defined as N. In order to look into the wear mechanisms, worn surface morphologies of layers were investigated using optical and scanning electron microscopy (OM and SEM).

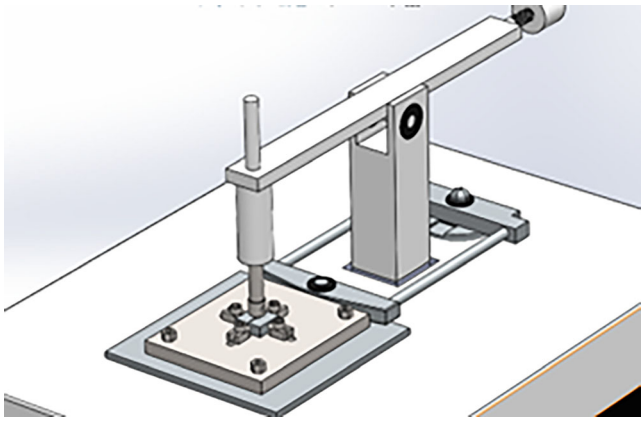

FIGURE 3 Reciprocating wear test instrument.

3 | RESULTS AND DISCUSSIONS

XRD patterns of PE and its layers are presented in Figure 4A–D. The diffraction peaks of PE were found at $2\theta^\circ = 21.5^\circ$ and 23.8° which correspond to the (110) and (200) diffraction planes in the orthorhombic phase of semi-crystalline PE.[8,27] As shown in Figure 4, the XRD patterns of all layers showed diffraction peaks at similar $2\theta^\circ$ values with PE. It was determined that the peaks of the (110) and (200) planes shifted to the right from the inside Figure 4A–D of all layers. In the XRD analysis of hydroxyapatite/polylactic acid composites, Nejati et al.[28] attributed the shifts in the peaks and changes in crystalline size to the presence of interactions between the filler and matrix. Peaks for GNP were seen in PE/GNP layers (Figure 4A) and in PE/GNP-GO hybrid layers (Figure 4D), which were connected to the graphitic (002) plane by the $2\theta^\circ = 26.7^\circ$ value.[29] The diffraction intensities of GNP peaks improved with increasing GNP wt%. According to Ma et al.,[30] larger GNP levels in epoxy matrix nanocomposites resulted in a higher diffraction intensity, which revealed the graphene layers in the diffraction (002) plane at $2\theta^\circ = 26.6^\circ$. Reddy et al.[31] reported the reason for the low intensities of the graphitic carbon peaks. Because the (110) and (200) diffraction planes were more intense than those of graphitic carbon. The amorphous content manifested as a broad peak around 19.6° in all layers. This peak was more intense in layers containing GO (Figure 4B). This result was attributed to the dominance of the amorphous region of the polymer.[32] These peaks showed that the composite layers exhibited a semi-crystalline structure like an unfilled polymer.[33] The XRD examination results of PE/GO layers did not show the characteristic peaks of GO, and the outcome showed that GO was completely exfoliated within the layer. And also, the dominant structure in all PE/CNT layers was the semicrystalline structure (Figure 4C). A similar result was reported with XRD analysis by Showkat et al.[34] They examined the crystal structures of composites prepared with poly (diphenyl amine) (PDPA) and multiwalled carbon nanotubes (MWNT), and found that the planar structure of PDPA was dominant rather than the hexagonal surface lattice of MWNT.

The values of crystalline size of layer are shown in Figure 5A. In comparison to PE, all filler components showed a decrease in the (110) and (200) planes at crystalline size values. According to Figure 5, layers with 3.0 wt%, GNP, 3.0 wt% GO, 3.0 wt%, GNP-GO, and 2.0 wt% CNT

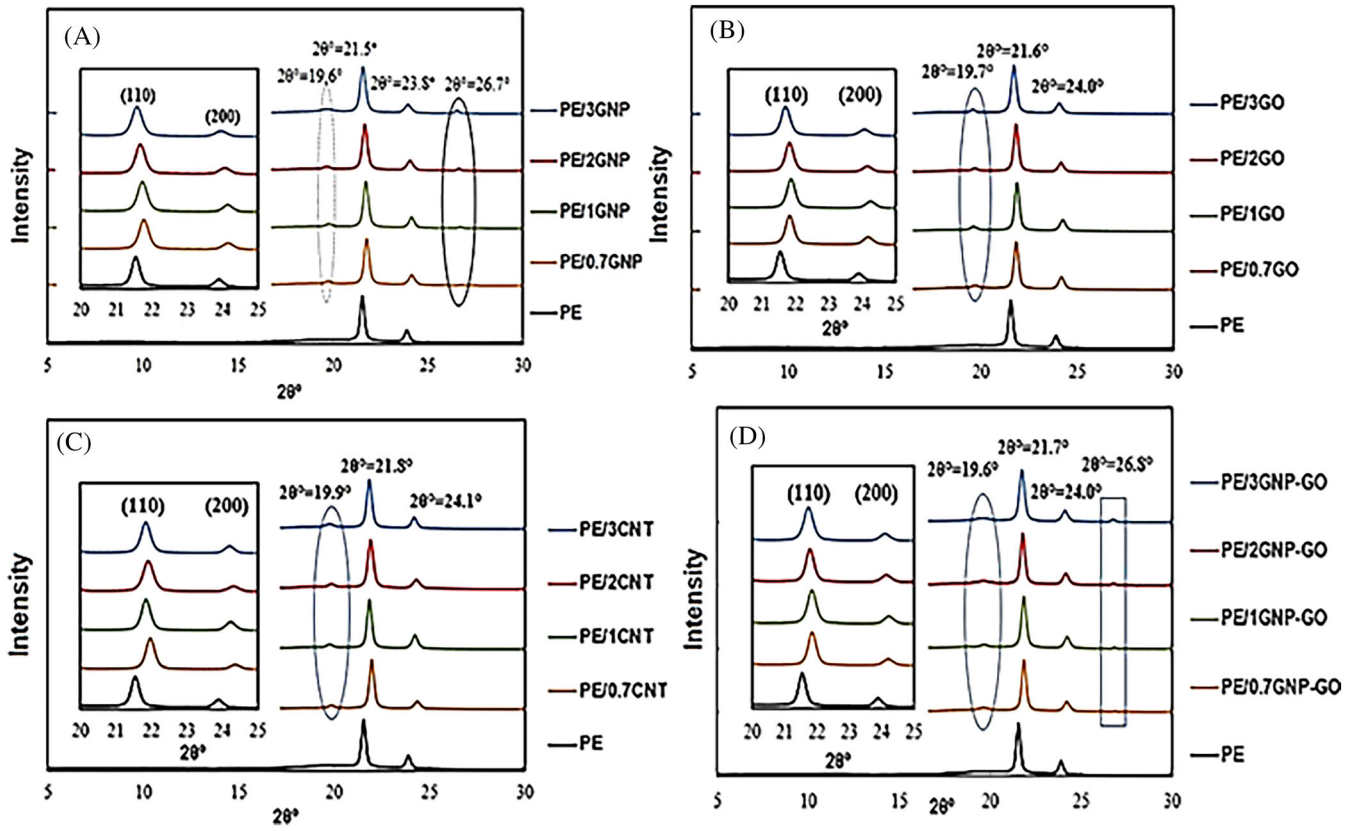

FIGURE 4 XRD diffractograms of PE and layers with graphene derivatives.

added to the polymer matrix displayed the lowest value. The inclusion of filler particles, which produce crystal defects, dislocations, and bind polymer chains, was blamed for the reduction in crystallite size.[16,18] As can be seen from Figure 5, the samples containing GNP at all filler contents and for both two planes showed the lowest crystalline size values. This situation is explained by the structures of GNP, GO, and CNT fillers. Although GNP and CNT are nanosized, GNP has a higher surface area than GO but is lower than CNT. The distribution of GNP in the matrix and its interaction with the polymer suggest that it binds polymer chains more than GO and CNT. Similar results found in this study and the literature were attributed to geometric differences between GNP and CNT.[35,36] Furthermore, as described in recent literature comparing various nanofiller materials, the applications of GNP and GO nanofiller materials are more promising than those of CNT.[37] In a newly published study examining polymer chain conformations in GNP/MWCNT filled UHMWPE hybrid composites, it was reported that GNP inhibits polymer chain movement more than CNT.[38] The XRD analysis results of this study showed that the intensity increased in the graphitic carbon peaks of GNP at high GNP content (Figure 4A). The GNP filler bound the crystalline regions of the polymer, revealing the amorphous regions. This result is proven by the decreases in crystal size values and the decreases observed in the band intensities of CH_2 and C—O groups in FTIR analysis results (Figure 8). These PE-GNP molecular interaction described are shown in Figure 5B. Figure 5C,D presents the low and high HR-TEM cross-section images of the PE/3GNP layer to demonstrate the interfacial interaction of GNP and PE. As can be seen in Figure 5C, the GNP layers got closer to each other, forming a continuous interconnected network, and dark areas and nearly transparent areas were observed on the cross-section surface of the PE/3GNP layers.

According to the literature, a continuous interconnected network is evident of homogenous dispersion of GNPs in the polymer matrix.[39,40] In the high-magnification HR-TEM image of the same layer in transparent areas (Figure 5D), a flaky morphology that is characteristic of the exfoliated structure[41] was observed. HR-TEM analysis performed on the cross-section confirmed the strong interfacial adhesion of the PE/3GNP layer due to the homogeneously distributed graphene layers. Previous polymer composite studies with GNP have also reported similar images.[42]

Figure 6 displays the FE-SEM images of PE and layer surfaces that were chosen based on crystalline size values, and EDS elemental maps are utilized to analyze the

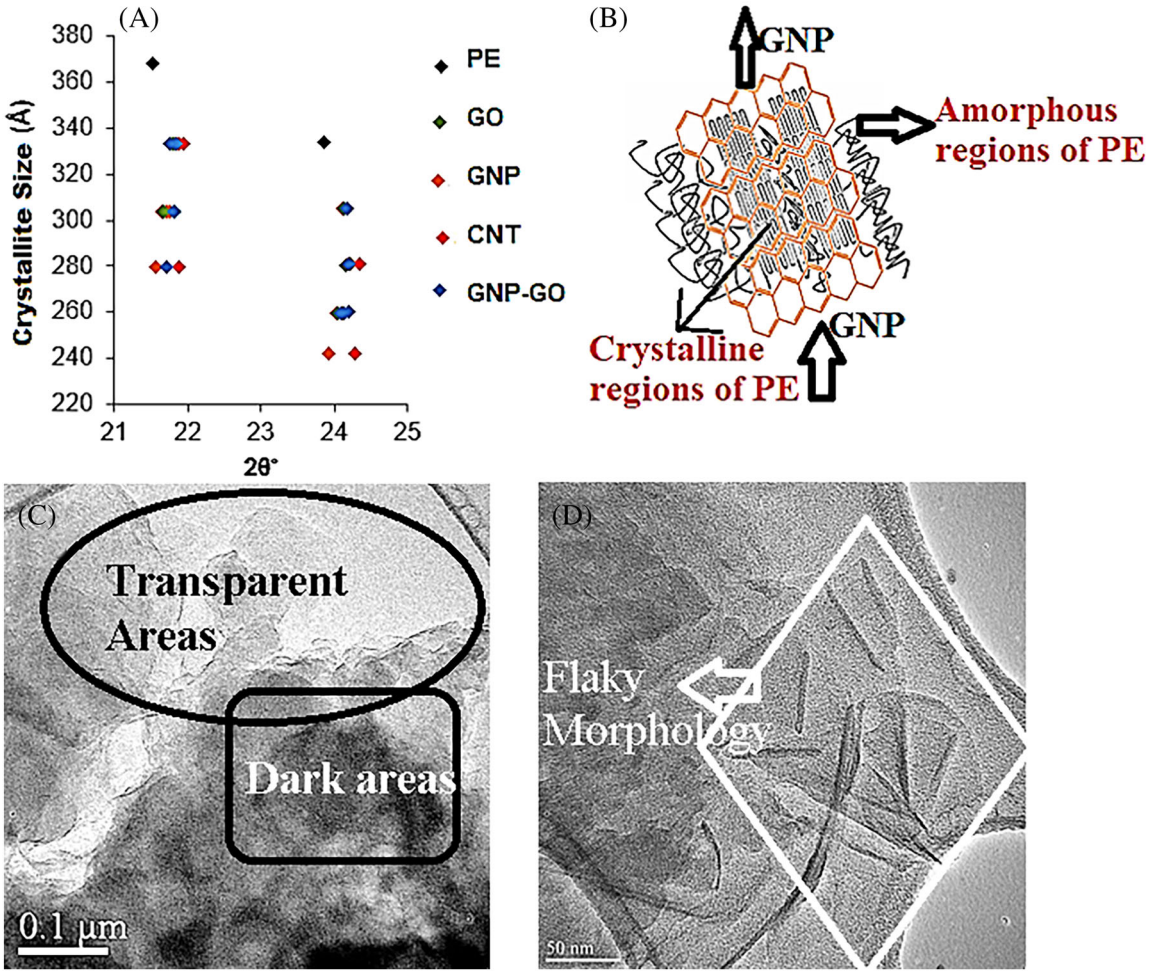

FIGURE 5 (A) Crystalline size values of layers with graphene derivatives, (B) PE-GNP molecular interaction representation according to the analysis results of this study, (C) low-magnification HR-TEM images of cross section area of PE/3GNP, and (D) the high-magnification HR-TEM images of cross section area of PE/3GNP.

distribution of oxygen in the polymer matrix. The surface structure of PE was relatively smooth similar to the literature.[17] The surface image of the PE/2GO composite layer, which had the highest crystal size value in both planes among the other layers, was mostly flat but consists of wrinkled surfaces at certain regions at Figure 6. And also, PE/1GNP, PE/1GNP-GO, and PE/2CNT films had a rough surface morphology. The images ordered according to the decreasing crystalline size values in Figure 6 showed that the surface structures became more and more heterogeneous. These images revealed that the filler materials caused a decrease in crystallinity by binding the polymer chains just like in XRD analysis. The oxygen groups of GO were equally distributed in the PE matrix, according to the results of the EDS elemental mapping for the PE/GO and PE/GNP-GO layers. The oxygen elements were shown on the EDS maps as red dots.

To reveal the crystalline structures, the surfaces of PE and layers were treated with acid etching (7% potassium permanganate/concentrated sulfuric acid). OM observed the treated and untreated surface structures in Figure 7. As can be seen from Figure 7, there are distinct and more bright regions on the surface of PE compared to other layers. There were traces showing the presence of dark and generally dotted crystal regions on the entire surface after etching.[43] The etched surface image of PE supported the XRD analysis results (Figure 4), which showed higher crystal size values than all composite and hybrid composite layers. Bright white regions were not very clearly visible in the unetched surface images of GNP, GO, CNT, and GNP-GO filled layers compared to PE. However, the darkened areas became evident due to the filler materials added to the matrix after etching.

FTIR spectrums of PE and layers are presented in Figure 8. The bands were seen at 2917.42–2849.37 cm^{-1} in Figure 8. The asymmetric and symmetric stretching vibrations of the CH_2 group were cited as the causes of these bands, respectively.[44] The characteristic bands of PE at 1464.04 and 719.27 cm^{-1} could be assigned to

CH_2 bending and CH_2 rocking stretching vibrations, respectively.[45] PE is defined by these peaks in the literature.[46] However, in this study, the presence of C—O vibration peaks at 1262.27, 1092.65, and 1025.35 cm^{-1} were clearly observed in the PE spectrum. The presence of oxygen groups in the structure resulting from the production of PE.[47] As seen from Figure 8A,C,D, the intensity of all vibration peaks (CH_2 asymmetric and symmetric, CH_2 bending, CH_2 rocking, and C—O groups stretching vibrations) of the PE/2GNP-PE/3GNP, PE/2CNT, and PE/2GNP-GO layers decreased compared to both PE and other layers. This observed change was due to interactions between matrix-filler[40] and the occurrence of new bonds.[48] As seen from the FTIR spectrum of PE/GNP layers at 2.0% and 3.0% GNP contents, it was understood that the interaction of both CH_2 groups and C—O groups with GNP was high due to the nano size and high surface area of GNP. The severe intensity reductions observed in the FTIR spectrum of the PE/2CNT layer sample, which gave the lowest crystalline size value in the XRD analysis results, reveal that this filler type and its amount affect the crystal regions in the polymer matrix. Also, the FTIR spectrum of PE/CNT layers has shown that the CNT additions also surround the polymer chain parts to which the oxygen groups are attached and reduce the vibrations. In the FTIR spectra of PE/GO

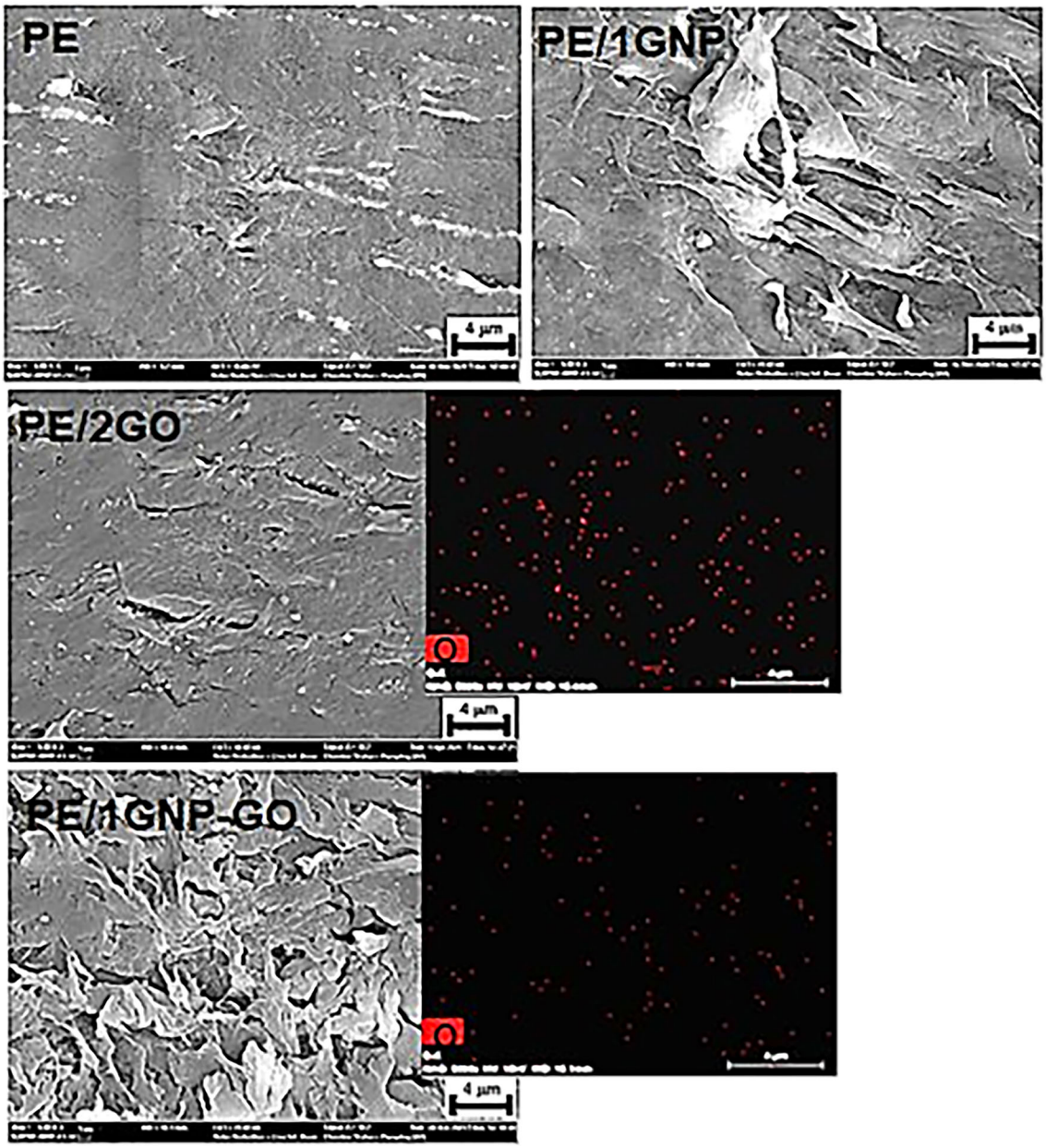

FIGURE 6 FE-SEM images of the surfaces of PE and layers and EDS elemental mapping results of PE/GO and PE/GNP-GO layers.

layers, it was determined that the peak intensities of C—O stretching vibrations decreased after 1.0% GO content, and no change was observed in the CH_2 group peaks. This result is an indication that GO, which has functional groups containing oxygen, enters between the polymer chains and causes interaction or the formation of a new bond. Intensity losses were observed in the FTIR spectra of PE/GNP-GO hybrid layers with the addition of 2.0% and 3.0% GNP-GO, and they gave results compatible with the FTIR spectra of hybrid layers prepared with only GNP.

The variation of the friction coefficient values obtained as a result of the wear tests of PE and layers according to distance is shown in Figure 9. As can be seen from Figure 9, it was understood that the friction behavior of PE was quite unstable, increasing to a higher level with increasing sliding distance. The reason was that the contact area increased with the sliding distance and the surface of the PE softened with the friction heat, thus causing an increase in the friction coefficient.[49] The average friction coefficient of PE was 0.197; the average friction coefficient values of PE/0.7GNP, PE/1GNP, PE/2GNP, and PE/3GNP composite layers were found to be 0.190, 0.218, 0.172, and 0.163, respectively. This friction coefficient value of PE was consistent with the literature.[50] However, the low friction coefficient values in PE/0.7GNP, PE/2GNP, and PE/3GNP composite layers were not observed in the study by Aliyu et al.[12] for PE/GNP composite materials. The friction coefficient of PE was determined at 0.15; the friction coefficient increased to 0.24 with the addition of GNP to the matrix. They attributed this increase to the fact that GNP addition prevents polymer chains from slipping over each other. In this study, the GNP (0.7, 2.0, and 3.0 wt%) additions decreased the friction coefficient values due to the additional lubricating effect of polymer chains on each other and the GNP–polymer interaction. However, the PE/1GNP composite layer had a higher friction coefficient value than the pure polymer. Huang et al.[51] reported high friction coefficient values in their study. They examined the tribological properties of PE composites with GO, and they concluded that the wrinkled and rough surface of the composite affected the mechanical properties. In this study, the FE-SEM surface image of the PE/1GNP composite layer given in Figure 5 was rather rough compared to the surface image of PE. Among the layers containing GO, the lowest friction coefficient value was observed in the PE/0.7GO (0.033) layer with the lowest GO content. The friction coefficient values of PE/1GO (0.086) and PE/3GO (0.072) layers were found to be lower than those of PE (0.197). This showed that the GO filler was homogeneously distributed in the matrix and had a lubricating effect.[6] Although an unstable change was observed in the variation of the friction coefficient depending on the sliding distance of the PE/2GO layer, the friction

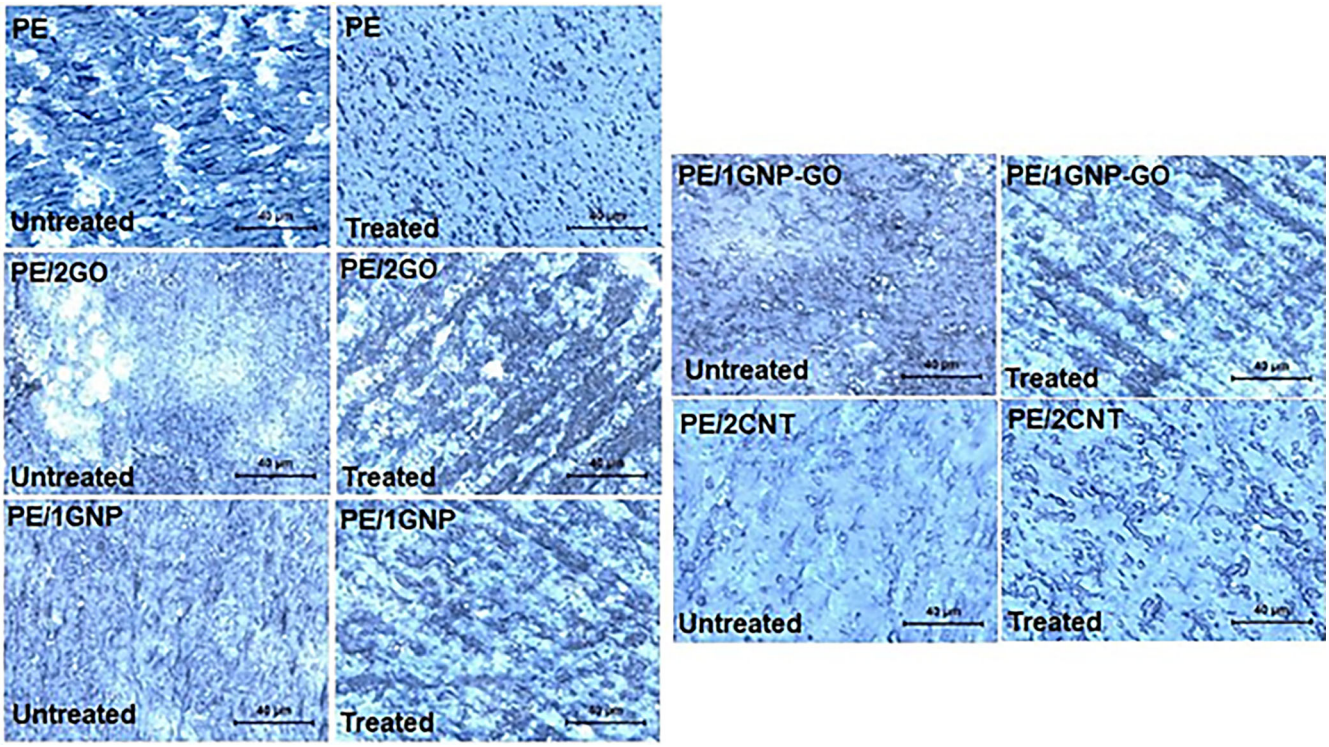

FIGURE 7 OM untreated and treated surface images of PE and layers with graphene derivatives.

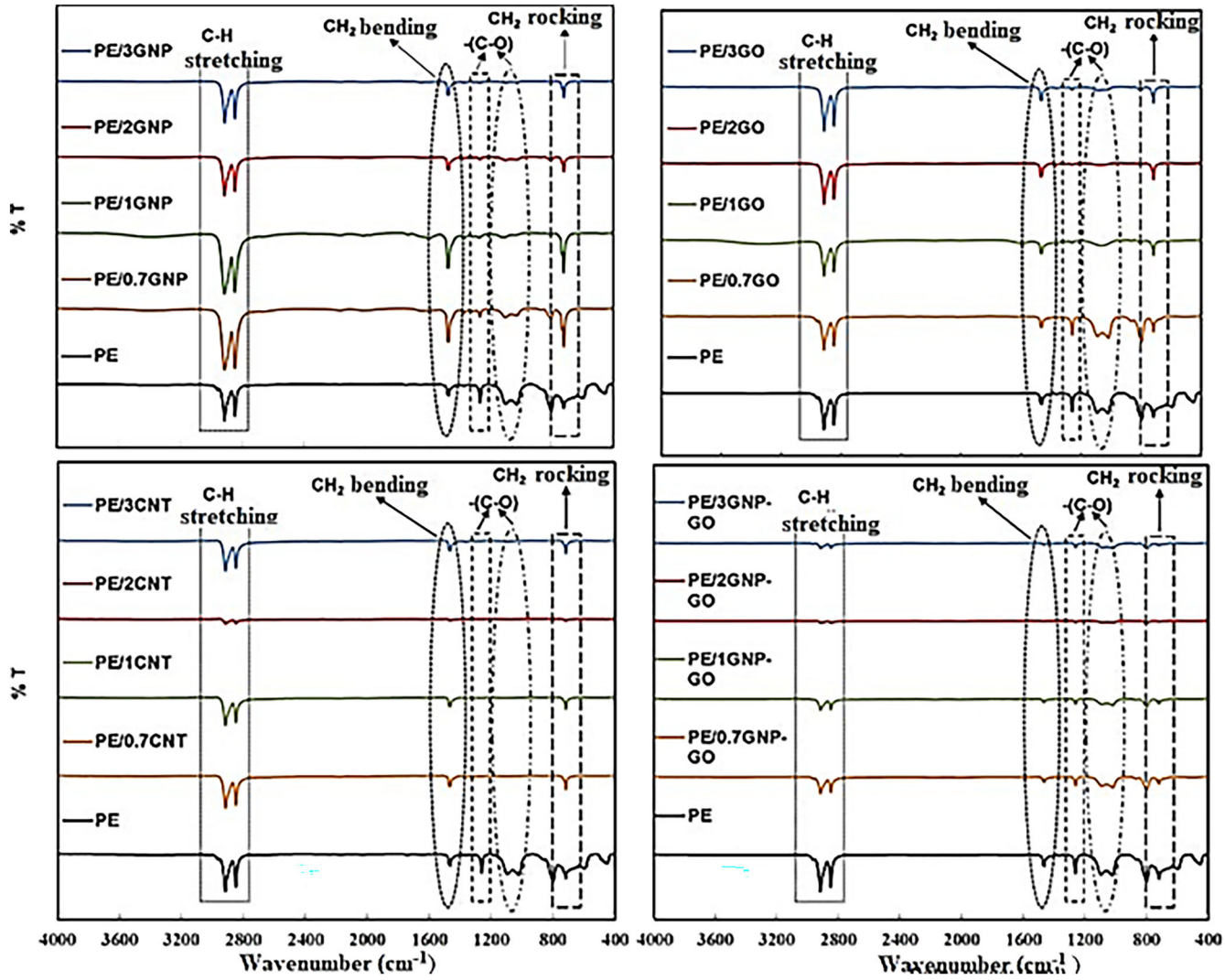

FIGURE 8 FTIR spectrums of PE and layers with graphene derivatives.

coefficient value was lower than that of the PE since the PE/2GO layer presented a flat appearance. Huang et al.[51] and Tai et al.[15] examined the tribological properties of PE composites with GO and reported that GO reduced the adhesion and friction force between the contact surfaces because it was a good solid lubricant. In the study of Huang et al.,[51] they found that the friction coefficient values of composites with GO were higher than the pure polymer. GO did not show lubricating properties due to the increase in lateral force. Tai et al.[15] reported that the friction coefficient increased because the GO was not distributed homogeneously in the polymer matrix. Although the lowest friction coefficient value among CNT layers was seen in PE/2CNT (0.182), the friction coefficients of PE/0.7CNT (0.186) and PE/1CNT (0.188) layers were also very close to each other. The highest friction coefficient value of PE/3CNT (0.194) had almost the same result as the friction coefficient value of the PE (0.197) in the layer. This decrease in friction coefficient with the addition of CNT was attributed to the fact that the CNT act as solid lubricants due to their smooth cylindrical surfaces that provide rolling motion during wear.[20] The friction coefficient values of the layers with GNP and GO were compared with the friction coefficients of the layers containing CNT, it was determined that nano-sized CNT and GNP additions gave values close to those of the PE, while the layers with GO had much smaller friction coefficient values. Based on these results, it was concluded that the lubricating effect of GO is stronger than that of both nano additives. As can be seen from Figure 9, the coefficients of friction of all hybrid layers were lower than those of PE but showed an unstable change compared to PE and composite layers because they contained a mixture of two fillers with different dimensions. However, this

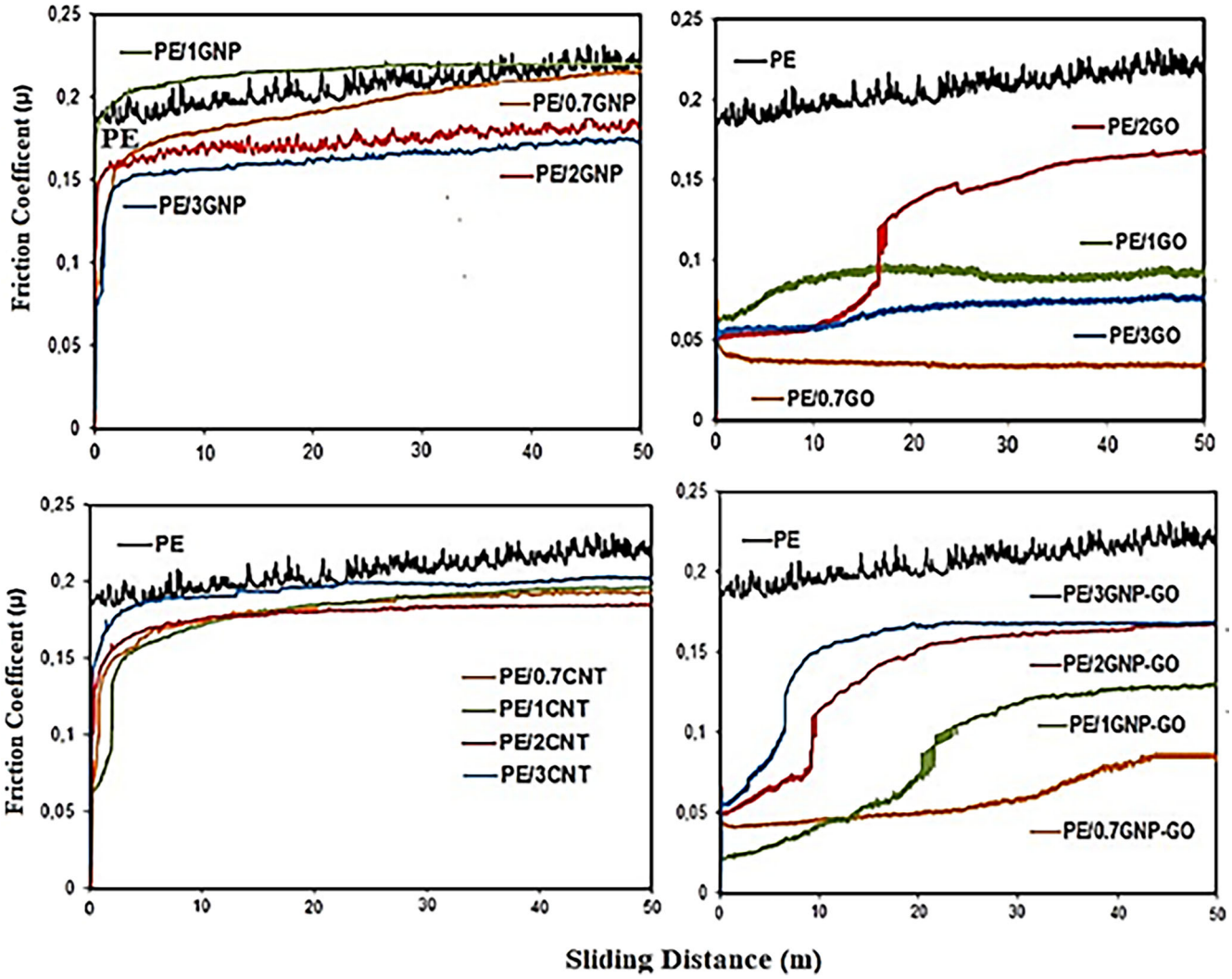

FIGURE 9 Friction coefficient values of PE and layers with graphene derivatives.

unstable change gave consistent results despite the increase in the amount of additive. PE/0.7GNP-GO hybrid composite layer showed the lowest and most stable coefficient of friction. After about 33 m, a change with a sudden increase was observed. However, with the increase in the amount of filler in other hybrid composites, both the friction coefficient and sudden changes were experienced at gradually lower distances. These results showed that the synergistic effect of the filler content added in the lowest amount in the hybrid composite layer was stronger. It had been determined that both GNP and GO had lubricating properties in composite and hybrid layers, individually or together.[52]

According to wear volume values, it was determined that the layers containing 3.0% GNP (0.02073 mm^3) and 1.0% GO (0.02111 mm^3) were the best filler and filler amounts to improve the wear resistance of PE (0.02378 mm^3). The decrease in wear rate observed in previous studies on PE composites was attributed to the lubricant properties of graphene,[17] the high aspect ratio, and the large surface area.[12] FTIR analysis results supported the improvement in wear resistance of the PE/3GNP and PE/1GO composites because they had the highest polymer-filler interaction (Figure 7). Kanagaraj et al.[50] attributed the decrease in wear volume of CNT-added polymer composites to load transfer depending on the polymer-CNT interface strength. Kumar et al.[19] reported that the addition of CNT played an important role in the tribological performance by increasing the crystallinity of the structure. It was concluded that the crystal phase would provide good damping by distributing the applied load; therefore, increasing crystallinity facilitates the energy dissipation mechanism and reduces the wear rate. In this study, it is thought that it is not correct to attribute the increase in wear rate to

the lack of interaction between CNT and polymer. Because the FTIR analysis results of the CNT-containing layers proved the existence of interactions (Figure 7). However, FE-SEM surface images and unetched and etched OM surface images, which were examined to obtain information about the crystallinity of the layers, showed that the layer with the least crystal structure compared to the other layers was the layer containing CNT. Therefore, the reason for the increase in the wear volume (0.04044 mm^3) indicates that the CNT did not affect the structure sufficiently to increase the crystallinity. The PE/1GNP-GO hybrid layer had the close wear volume value (0.02423 mm^3) as the PE (0.02378 mm^3). The wear volume values of hybrid layers (0.02796 mm^3—PE/0.7GNP-GO; 0.02600 mm^3-PE/2GNP-GO; 0.02740 mm^3—PE/3GNP-GO) were higher than the values of all GO containing layers (0.02275 mm^3—PE/0.7GO; 0.02462 mm^3—PE/2GO; 0.02484 mm^3—PE/3GO). And, hybrid layers showed higher values compared to layers containing 2.0 wt% (0.02323 mm^3) and 3.0 wt% GNP (0.02073 mm^3) but lower values than layers containing 0.7 wt% (0.03101 mm^3) and 1.0 wt% GNP (0.02592 mm^3). According to these results, it was concluded that there is a synergistic effect of both GO and GNP on wear properties.

FE-SEM images of worn surface of PE and layers and OM images of their corresponding testing balls are shown in Figure 10. The FE-SEM surface images of PE showed a deep grooved, wavy structure perpendicular to the slip direction, which was the typical indicator of fatigue wear. Many microscopic fluctuations on the worn surface of PE under dry wear conditions had been attributed to the heat softening of the polymer matrix during friction.[49] In addition, the presence of microcracks at the bottom of the deep grooves was also observed in Figure 10. These microcracks and a large amount of scattered wear debris both in the center and around the ball showed that fatigue wear was the dominant wear mechanism in the PE.[17] It was determined that abrasive wear and fatigue wear tracks on the worn surface of the PE/3GNP composite layer were significantly reduced compared to PE. The relatively smooth worn surface of the PE/3GNP composite layer that had the lowest wear rate results and the best GNP-polymer interaction were observed. 3.0 wt% GNP addition was the amount that offered the most advantageous results for the PE matrix.[17] There were adhesive wear traces but no fatigue traces in the worn surface of the PE/1GO layers with the lowest wear rate value. Also, the ball surface wear products appeared to be quite minimal. As a result, it was understood that a 1.0 wt% GO addition was the maximum amount that improved wear resistance. Li et al.[53] reported that the loads are transferred and carried at larger forces due to the two-dimensional structure of GO.

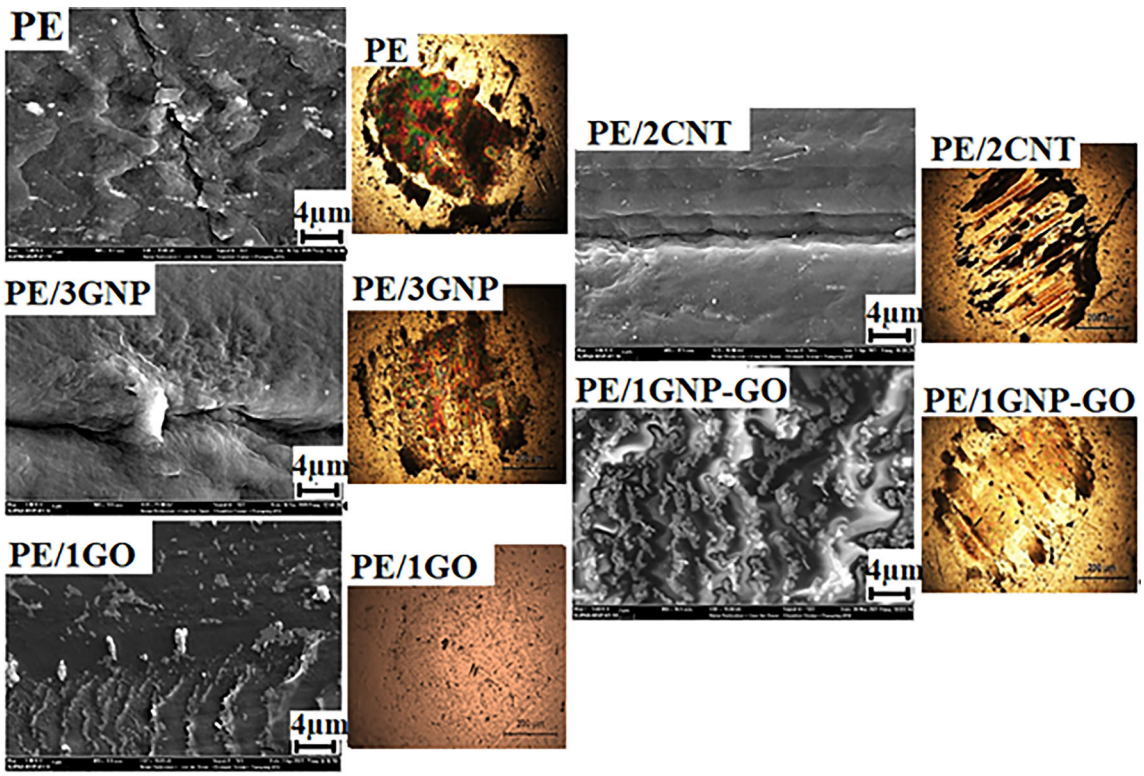

FIGURE 10 FE-SEM images of worn surface of PE and layers and OM images of their corresponding testing balls.

4 | CONCLUSIONS

In this paper, all composite powders were prepared by liquid-phase mixing of carbon derivative colloids with PE matrix, and then composite and hybrid composite layers were produced by hot press molding. XRD analysis results confirmed the semi-crystalline structure of all layers, just like PE. The decrease in crystallite size values was attributed to binded polymer chains at the highest filler amounts. The PE/2GO composite layer had the highest crystal size value in both planes among the other layers, according to the etched surface image and crystal size values. Among all fillers, layers containing GO gave the lowest friction coefficient values. The friction coefficient in the PE/0.7GO (0.033) composite layer was reduced by 83.24% as compared to PE (0.197). The PE/3GNP and PE/1GO layers increased the wear resistance of PE by 12% and 11%, respectively. Dry wear test results showed that PE/1GO and PE/3GNP composite layers were wear-resistant layers. And these results were attributed to the lubricant properties, the high aspect ratio, the large surface area of graphene, and the homogeneous distribution of graphene in the matrix. These results revealed that nano-sized GNP provided an effective charge transfer and that GO filler was homogeneously distributed in the matrix.

ACKNOWLEDGMENTS

The authors thank the financial support of the research foundation (Project no: 2020-02.BŞEÜ.03-04) of Bilecik Şeyh Edebali University.

DATA AVAILABILITY STATEMENT

Data are available on request from the authors.

ORCID

Ferda Mindivan https://orcid.org/0000-0002-6046-2456
Hilal Dere https://orcid.org/0000-0002-0658-3134

REFERENCES

1. Gu J, Li N, Tian L, Lv Z, Zhang Q. High thermal conductivity graphite nanoplatelet/ UHMWPE nanocomposites. *RSC Adv*. 2015;5:36334-36339.
2. Dayyoub T, Maksimkin AV, Kaloshkin S, et al. The structure and mechanical properties of the UHMWPE films modified by the mixture of graphene nanoplates with polyaniline. *Polymers*. 2019;11:23.
3. Kurtz SM. A primer on UHMWPE. *UHMWPE Biomaterials Handbook*, ELSEVIER. 3rd ed., 2016:1-6.
4. Melk L, Emami N. Mechanical and thermal performances of UHMWPE blended vitamin E reinforced carbon nanoparticle composites. *Compos B: Eng*. 2018;146:20-27.
5. Pang W, Ni Z, Chen G, Huang G, Huang H, Zhao Y. Mechanical and thermal properties of graphene oxide/ultrahigh molecular weight polyethylene nanocomposites. *RSC Adv*. 2015;5:63063-63072.
6. An Y, Tai Z, Qi Y, et al. Friction and wear properties of graphene oxide/ultrahigh-molecularweight polyethylene composites under the lubrication of deionized water and normal saline solution. *J Appl Polym*. 2014;131:39640.
7. Çolak A, Göktaş M, Mindivan F. Effect of reduced graphene oxide amount on the tribological properties of UHMWPE biocomposites under water-lubricated conditions. *SN Appl Sci*. 2020;2:375.
8. Alam F, Choosri M, Gupta TK, Varadarajan KM, Choi D, Kumar S. Electrical, mechanical and thermal properties of graphene nanoplatelets reinforced UHMWPE nanocomposites. *Mater Sci Eng B*. 2019;241:82-91.
9. Nieto A, Lahiri D, Agarwal A. Synthesis and properties of bulk graphene nanoplatelets consolidated by spark plasma sintering. *Carbon*. 2012;50:4068-4077.
10. Lahiri D, Dua R, Zhang C, et al. Graphene nanoplatelet-induced strengthening of ultrahigh molecular weight polyethylene and biocompatibility in vitro. *ACS Appl Mater Interfaces*. 2012;4:2234-2241.
11. Wang B, Li H, Li L, Chen P, Wang Z, Gu Q. Electrostatic adsorption method for preparing electrically conducting ultrahigh molecular weight polyethylene/graphene nanosheets composites with a segregated network. *Compos Sci Technol*. 2013;89:180-185.
12. Aliyu IK, Mohammed AS, Al-Qutub A. Tribological performance of ultra high molecular weight polyethylene nanocomposites reinforced with graphene nanoplatelets. *Polym Compos*. 2018;40:E1301-E1311.
13. Chih A, Ansón-Casaos A, Puértolas JA. Frictional and mechanical behavior of graphene/UHMWPE composite coatings. *Tribol Int*. 2017;116:295-302.
14. Tahriri M, Del Monico M, Moghanian A, et al. Graphene and its derivatives: opportunities and challenges in dentistry. *Mater Sci Eng C*. 2019;102:171-185.
15. Tai Z, Chen Y, An Y, Yan X, Xue Q. Tribological behavior of UHMWPE reinforced with graphene oxide nanosheets. *Tribol Lett*. 2012;46:55-63.
16. Chen Y, Qi Y, Tai Z, Yan X, Zhu F, Xue Q. Preparation, mechanical properties and biocompatibility of graphene oxide/ultrahigh molecular weight polyethylene composites. *Eur Polym J*. 2012;48:1026-1033.
17. Pang W, Ni Z, Wu J, Zhao Y. Investigation of tribological properties of graphene oxide reinforced ultrahigh molecular weight polyethylene under artificial seawater lubricating condition. *Appl Surf Sci*. 2018;434:273-282.
18. Cividanes LS, Simonetti EAN, Moraes MB, Fernandes FW, Thim GP. Influence of carbon nanotubes on epoxy resin cure reaction using different techniques: a comprehensive review. *Polym Eng Sci*. 2014;54:2461-2469.
19. Kumar MR, Rajesh K, Haldar S, et al. Surface modification of CNT reinforced UHMWPE composite for sustained drug delivery. *J Drug Deliv Sci Technol*. 2019;52:748-759.
20. Kumar RM, Sharma SK, Kumar BVM, et al. Effects of carbon nanotube aspect ratio on strengthening and tribological behavior of ultra high molecular weight polyethylene composite. *Compos Part A*. 2015;76:62-72.
21. Zoo YS, An JW, Lim DP, Lim DS. Effect of carbon nanotube addition on tribological behavior of UHMWPE. *Tribol Lett*. 2004;16:305-309.

22. Samad MA, Sinha SK. Mechanical, thermal and tribological characterization of a UHMWPE film reinforced with carbon nanotubes coated on steel. *Tribol Int*. 2011;44:1932-1941.
23. Hummers WS, Offeman RE. Preparation of graphitic oxide. *J Am Chem Soc*. 1958;80:1339.
24. Dere H. Friction and wear behaviors of carbon derivative filled ultra high molecular weight polyethylene (PE) composite and hybrid composite layers. Master Thesis BSEU, Turkey. 2021.
25. Monshi A, Foroughi MR, Monshi MR. Modified scherrer equation to estimate more accurately nano-crystallite size using XRD. *World J Nano Sci Eng*. 2012;2:154-160.
26. Danilchenko SN, Kukharenko OG, Moseke C, Protsenko IY, Sukhodub LF, Sulkio-Cleff B. Determination of the bone mineral crystallite size and lattice strain from diffraction line broadening. Protsenko IY, Sukhodub LF, Sulkio-Cleff B. *Cryst Res Technol*. 2002;37:1234-1240.
27. Mohammed AS, Ali A, Nesar M. Evaluation of tribological properties of organoclay reinforced UHMWPE nanocomposites. *J Tribol*. 2017;139:012001.
28. Nejati E, Firouzdor V, Eslaminejad MB, Bagheri F. Needle-like nano hydroxyapatite/poly(L-lactide acid) composite scaffold for bone tissue engineering application. *Mater Sci Eng C*. 2009;29:942-949.
29. Turan ME, Sun Y, Akgül Y, et al. The effect of GNPs on wear and corrosion behaviors of pure magnesium. *J Alloys Compd*. 2017;724:14-23.
30. Ma J, Meng Q, Zaman I, et al. Development of polymer composites using modified, high-structural integrity graphene platelets. *Compos Sci Technol*. 2014;91:82-90.
31. Reddy SK, Kumar S, Varadarajan KM, Marpu PR, Gupta TK, Choosri M. Strain and damage-sensing performance of biocompatible smart CNT/ UHMWPE nanocomposites. *Mater Sci Eng C*. 2018;92:957-968.
32. Kolanthai E, Bose S, Bhagyashree KS, et al. Graphene scavenges free radicals to synergistically enhance structural properties in a gamma-irradiated polyethylene composite through enhanced interfacial interactions. *Phys Chem Chem Phys*. 2015;17:22900-22910.
33. Shi W, Dong H, Bell T. Tribological behaviour and microscopic wear mechanisms of UHMWPE sliding against thermal oxidation-treated Ti6Al4V. *Mater Sci Eng A*. 2000;291:27-36.
34. Showkat AM, Lee KP, Gopalan AI, et al. Characterization and preparation of new multiwall carbon nanotube/conducting polymer composites by in situ polymerization. *J Appl Polym Sci*. 2006;101:3721-3729.
35. Ren Y, Zhang L, Xie G, et al. A review on tribology of polymer composite coatings. *Friction*. 2021;9:429-470.
36. Tao J, Wang J, Zeng Q. A comparative study on the influences of CNT and GNP on the piezoresistivity of cement composites. *Mater Lett*. 2020;259:126858.
37. Sobhani E, Avcar M. The influence of various nanofiller materials (CNTs, GNPs, and GOPs) on the natural frequencies of nanocomposite cylindrical shells: a comparative study. *Mater Today Commun*. 2022;33:104547.
38. Fu C, Zhang R, Tian J, Yang Q, Xue P, Chen X. Polymer chain conformations in hybrid composites of UHMWPE incorporated by GNP/MWCNT. *J Polym Res*. 2023;30(6):245.
39. Inuwa IM, Hassan A, Samsudin SA, et al. Characterization and mechanical properties of exfoliated graphite nanoplatelets reinforced polyethylene terephthalate/polypropylene composites. *J Appl Polym Sci*. 2014;131(15):1-9.
40. Han Z, Wang Y, Dong W, Wang P. Enhanced fire retardancy of polyethylene/alumina trihydrate composites by graphene nanoplatelets. *Mater Lett*. 2014;128:275-278.
41. Liu T, Li B, Lively B, Eyler A, Zhong WH. Enhanced wear resistance of high-density polyethylene composites reinforced by organosilane-graphitic nanoplatelets. *Wear*. 2014;309(1–2):43-51.
42. Yang B, Pan Y, Yu Y, et al. Filler network structure in graphene nanoplatelet (GNP)-filled polymethyl methacrylate (PMMA) composites: from thermorheology to electrically and thermally conductive properties. *Polym Test*. 2020;89:106575.
43. Mindivan F, Çolak A. Tribo-material based on a UHMWPE/RGOC biocomposite for using in artificial joints. *J Appl Polym Sci*. 2021;138:50768.
44. Macuvele DLP, Colla G, Cesca K, et al. UHMWPE/HA biocomposite compatibilized by organophilic montmorillonite: An evaluation of the mechanical-tribological properties and its hemocompatibility and performance in simulated blood fluid. *Mater Sci Eng C*. 2019;100:411-423.
45. Meng L, Li W, Ma R, et al. Long UHMWPE fibers reinforced rigid polyurethane composites: An investigation in mechanical properties. *Eur Polym J*. 2018;105:55-60.
46. Chang BP, Akil HM, Nasir RB, et al. Optimization on wear performance of UHMWPE composites using response surface methodology. *Tribol Int*. 2015;88:252-262.
47. Poljansek I, Sebenik U, Krajnc M. Characterization of phenol–urea–formaldehyde resin by inline FTIR spectroscopy. *J Appl Polym Sci*. 2006;99:2016-2028.
48. Kandhol G, Wadhwa H, Chand S, Mahendia S, Kumar S. Study of dielectric relaxation behavior of composites of poly (vinyl alchohol) (PVA) and reduced graphene oxide (RGO). *Vacuum*. 2019;160:384-393.
49. Dangsheng X. Friction and wear properties of UHMWPE composites reinforced with carbon fiber. *Mater Lett*. 2005;59:175-179.
50. Kanagaraj S, Mathew MT, Fonseca A, Oliveira MSA, Simoes JAO, Rocha LA. Tribological characterisation of carbon nanotubes/ultrahigh molecular weight polyethylene composites: the effect of sliding distance. *Int J Surf Sci Eng*. 2010;4:305-321.
51. Huang G, Ni Z, Chen G, Zhao Y. The influence of irradiation and accelerated aging on the mechanical and tribological properties of the graphene oxide/ultra-high-molecular-weight polyethylene nanocomposites. *Int J Polym Sci*. 2016;2016:1-9.
52. Liu T, Wang Y, Eyler A, Zhong WH. Synergistic effects of hybrid graphitic nanofillers on simultaneously enhanced wear and mechanical properties of polymer nanocomposites. *Eur Polym J*. 2014;55:210-221.
53. Li X, Yue F, Pang W, Wu J, Kong B. Mechanical and wear properties of GO-enhanced irradiated UHMWPE with good oxidation resistance. *Fullerenes Nanotubes Carbon Nanostruct*. 2019;27:459-467.

How to cite this article: Mindivan F, Dere H. Wear-resistant layers containing graphene derivatives. *Polym Compos*. 2024;45(5):4138-4150. doi:10.1002/pc.28048